Published in final edited form as:
Exp Neurol. 2011 September ; 231(1): 171–180. doi:10.1016/j.expneurol.2011.06.005.

Insulin resistance impairs nigrostriatal dopamine function

J.K. Morris[1], **G.L. Bomhoff**[1], **B.K. Gorres**[1], **V.A. Davis**[5], **J. Kim**[4], **P-P Lee**[1,4], **W.M. Brooks**[2,4], **G.A. Gerhardt**[5], **P.C. Geiger**[1,3], and **J.A. Stanford**[1,3]

[1]Department of Molecular and Integrative Physiology, University of Kansas Medical Center, Kansas City, KS 66160

[2]Department of Neurology, University of Kansas Medical Center, Kansas City, KS 66160

[3]Kansas Intellectual and Developmental Disabilities Research Center, University of Kansas Medical Center, Kansas City, KS 66160

[4]Hoglund Brain Imaging Center, University of Kansas Medical Center, Kansas City, KS 66160

[5]Department of Anatomy and Neurobiology, University of Kentucky Chandler Medical Center, Lexington, KY 40536

Abstract

Clinical studies have indicated a link between Parkinson's disease (PD) and Type 2 Diabetes. Although preclinical studies have examined the effect of high-fat feeding on dopamine function in brain reward pathways, the effect of diet on neurotransmission in the nigrostriatal pathway, which is affected in PD and parkinsonism, is less clear. We hypothesized that a high-fat diet, which models early-stage Type 2 Diabetes, would disrupt nigrostriatal dopamine function in young adult Fischer 344 rats. Rats were fed a high fat diet (60% calories from fat) or a normal chow diet for 12 weeks. High fat-fed animals were insulin resistant compared to chow-fed controls. Potassium-evoked dopamine release and dopamine clearance were measured in the striatum using *in vivo* electrochemistry. Dopamine release was attenuated and dopamine clearance was diminished in the high-fat diet group compared to chow-fed rats. Magnetic resonance imaging indicated increased iron deposition in the substantia nigra of the high fat group. This finding was supported by alterations in the expression of several proteins involved in iron metabolism in the substantia nigra in this group compared to chow-fed animals. The diet-induced systemic and basal ganglia-specific changes may play a role in the observed impairment of nigrostriatal dopamine function.

Keywords

Parkinson's disease; insulin; glucose; diabetes; iron; high fat diet

Corresponding author: John A. Stanford, PhD, Kansas Life Sciences Innovation Center, Mail Stop 3051, 3901 Rainbow Boulevard, University of Kansas Medical Center, Kansas City, KS 66160, jstanford@kumc.edu, Main Phone Number: (913) 588-7416, Alternate Phone Number: (913) 588-9830, Fax Number: (913) 588-5677.

Introduction

Although much is understood about Parkinson's disease (PD) pathophysiology, its etiology remains unknown. Genes involved in processes as diverse as organelle trafficking, degradation pathways, and mitochondrial or antioxidant function are affected in PD (Sulzer, 2007). In addition, non-genetic factors, such as aging (Hindle, 2010), pesticide exposure (Priyadarshi et al., 2001, Priyadarshi et al., 2000), diet (Anderson et al., 1999, Johnson et al., 1999, Logroscino et al., 1996), adiposity (Abbott et al., 2002, Hu et al., 2006) and diabetes (Hu et al., 2007, Schernhammer et al., 2011, Xu et al., 2011) have been linked to PD. It is likely that both environmental and genetic factors contribute to dopamine (DA) neuron degeneration in PD.

Several clinical studies link PD with Type 2 Diabetes or obesity (Abbott et al., 2002, Hu et al., 2007, Hu et al., 2006, Schernhammer et al., 2011, Xu et al., 2011). Because over 80% of individuals with diagnosed Type 2 Diabetes are overweight or obese (Eberhardt, 2004), a high fat (HF) diet is often used to model diabetes preclinically. We and others have shown that a HF diet makes DA-producing neurons in the substantia nigra (SN) more vulnerable to toxin exposure (Choi et al., 2005, Morris et al., 2010). Furthermore, motor symptoms of PD are worse in individuals with co-morbid Type 2 Diabetes (Papapetropoulos et al., 2004), and diabetes is associated with more severe parkinsonian signs in aged individuals without PD (Arvanitakis et al., 2007). However, little is understood about the mechanisms by which a HF diet or Type 2 Diabetes put the brain at risk and what factors may contribute. Studies provide evidence of increased circulating iron levels in Type 2 Diabetes (Fernandez-Real et al., 2002, Rajpathak et al., 2009, Swaminathan et al., 2007), which is interesting because iron levels are also increased in the SN in PD patients (Rhodes and Ritz, 2008). It is possible that iron accumulation in DA neurons may contribute to nigrostriatal vulnerability and impaired function. In addition, it has been shown that short and long term HF feeding decreases DA release in striatal slices (Geiger et al., 2009, York et al., 2010). However, the extent to which a HF diet affects nigrostriatal DA function *in vivo* is unknown. Furthermore, important peripheral effects of HF feeding, such as glucose tolerance, insulin, or ghrelin levels, have not been characterized in the context of striatal DA function.

The purpose of this study was to analyze the degree to which HF diet-induced insulin resistance affects nigrostriatal DA function and iron deposition *in vivo*. In addition, we present a potential mechanism by which iron deposition could occur in this model. Measurement of potassium-evoked striatal DA release using *in vivo* electrochemistry allowed for calcium-dependent neurotransmitter release to be analyzed, mimicking normal neurotransmission, and for characterization of release dynamics across the dorsal striatum with a consistent stimulus in intact rats. Magnetic resonance imaging (MRI) permitted measurement of iron deposition *in vivo*, and iron transport proteins were measured in the SN using western blot. This study characterizes the role of HF-diet induced insulin resistance on nigrostriatal DA function and suggests a role for iron dysregulation in the SN.

Materials and Methods

Animals and Diet

Four-month-old male Fischer 344 rats were obtained from National Institutes on Aging colonies (Harlan). Rats were individually housed on a 12 hour light/dark cycle and provided food and water *ad libitum*. Rats in the control group (n=11) received chow (Harlan Teklad rodent diet 8604; 5% kCal from fat, 40% kCal from carbohydrate), while animals in the experimental group (n=15) received a HF diet (60% kCal from fat, 20% kCal from carbohydrate; Table 1) for 12 weeks. The composition of the HF diet has been described previously (Gupte et al., 2009). Food intake was measured every 2-3 days and body weight

was measured weekly. Protocols for animal use were approved by the University of Kansas Medical Center Institutional Animal Care and Use Committee and adhered to the Guide for the Care and Use of Laboratory Animals (National Research Council, 1996).

Materials

Rat insulin, ferritin, and unacylated ghrelin ELISA kits were purchased from ALPCO diagnostics (Salem, NH), while a glutathione assay was obtained from Oxford Biomedical Research (Oxford, MI). Carbon fiber electrodes were purchased from Quanteon, Inc (Lexington, KY). Primary antibody corresponding to transferrin (Tf) was purchased from Enzo Life Sciences (Plymouth Meeting PA), while anti-transferrin receptor 1 (TfR1) was obtained from Invitrogen (Carlsbad, California). Anti-phospho-AKT and total AKT were obtained from Cell Signaling Technology (Beverly, MA), while actin antibodies were purchased from Abcam (Cambridge, UK). Anti-transferrin receptor 2 (TfR2), anti-divalent metal transporter 1 (DMT1), and anti-ferroportin were purchased from Alpha Diagnostic (San Antonio, TX). All other chemicals were obtained from Sigma-Aldrich (St. Louis, MO).

Intraperitoneal glucose tolerance test (IPGTT)

An intraperitoneal glucose tolerance test (IPGTT) was performed one week prior to tissue harvest following a 12-hour fast. Before glucose injection, serum samples were collected to analyze fasting insulin and unacylated ghrelin. Tubes used to collect blood for analysis of ghrelin were coated with EDTA prior to serum collection. Blood was placed on ice for 10 minutes before centrifugation (20 min at 4°C). Serum was aliquoted into fresh tubes for analysis using ELISAs specific to insulin or unacylated ghrelin (ALPCO). At time t=0, a 60% glucose bolus was administered at 2g/kg body weight. Glucose was quantified in tail blood using a glucometer at six timepoints over the following 2 hrs as previously described (Morris et al., 2010).

Magnetic resonance imaging (MRI) image processing and analysis

High resolution MRI was performed using a 9.4 T Varian system equipped with a 12 cm gradient coil (40 G/cm, 250 μs) (Varian Inc., Palo Alto, CA). Animals were imaged using a 6 cm volume transmit radio frequency (RF) coil and a detunable surface receive RF coil. Anesthesia was induced by 4% isoflurane mixed with 4 L/min air and 1L/min O_2 and maintained by 1-1.5% isoflurane. Body temperature was maintained at 37°C using a circulating hot water pad and a temperature controller (Cole-Palmer, NY). Respiration was also monitored via a respiration pillow (SA Instruments, NY). T2 MRI was performed using a spin echo sequence with multiple echo times (TE). MRI parameters were TR/TE = 1200 / 13, 26, 39 and 52 ms, FOV = 3 × 3 cm, matrix = 256 × 256, slice thickness = 0.9 mm, number of averages = 4, and scan time per TE = 21 min. T2 maps were generated by fitting MR signal intensities to a mono-exponential function using a Simplex algorithm in ImageJ software (NIH) in a pixel-by-pixel basis.

Electrode preparation

Prior to the experiment, Ag/AgCl reference electrodes were plated by placing silver wire into a solution of 1M HCL saturated with NaCL while administering a current for 15 minutes. Reference electrodes were stored in 3M NaCl until use. Glass capillary micropipettes were prepared using a micropipette puller (KOPF instruments) and bumped to an inner diameter of 10 μm. Carbon fiber recording electrodes (30 μ O.D × 100 microns in length) were coated 2x with Nafion®, baked at 200°C for 4 minutes following each coat, and attached to a glass micropipette at a distance of 200 μm from electrode to micropipette tip with Stickywax. The morning of the experiment, recording electrodes were calibrated using stock solutions of 20mM DOPAC and 2mM DA added to 0.05M PBS (pH 7.4) to

determine sensitivity and selectivity for DA. All electrodes used exhibited a selectivity for DA of >300:1 vs. DOPAC, limit of detection of <0.01 μM and were linear to DA additions.

In vivo electrochemistry

Animals were anesthetized using urethane (1.25g/kg) over the course of three injections and placed into a stereotaxic frame. A prepared Ag/AgCl reference electrode was placed into the brain in an area distal to the striatum and a burr hole was drilled at striatal stereotaxic coordinates of 1.0 A/P and 3.0 M/L. Each carbon fiber recording electrode was lowered using a microdrive at 0.5mm/min into the striatum. *In vivo* chronoamperometric measurements were made using the FAST-16 system (Quanteon, L.L.C.). A square wave of 0.0V (resting potential) to +0.55V (applied potential) vs. the reference electrode was applied with a pulse duration of 100ms. A filtered potassium chloride (KCl) solution (70mM KCl, 79mMNaCl, 2.5mM $CaCl_2$, pH 7.4) was pressure ejected using a Picospritzer III (Parker instrumentation) and the volume ejected was carefully monitored through a MEIJI scope with a 10mm reticule. DA responses were evoked every 0.5mm from 2.0 mm to 5.0 mm and were averaged for each animal. Data were analyzed using FAST analysis software version 2.1. We based our *in vivo* electrochemistry signal parameters on those previously published (Hoffman and Gerhardt, 1998). For each rat, we obtained the following signal parameters: 1) amplitude / volume, the amplitude of the signal normalized to the amount of KCl (nL) infused to elicit the signal, 2) T_{80}, the time a signal decay to 80% of peak amplitude, and 3) T_c (clearance rate), the change in DA concentration between 20% (T_{20}) and 60% (T_{60}) of peak amplitude. It should be noted that T_{80} and T_c are specific to DA uptake and not diffusion or metabolism (Cass et al., 1993). Rise time for peak amplitude was also calculated for each signal in order to account for the potential influence of diffusion related to differences in parenchymal tortuosity between the two groups.

Measurement of circulating hormones and oxidative stress

Prior to tissue harvest, blood was collected for measurement of serum ferritin and oxidized and reduced glutathione. Blood for glutathione analysis was immediately stored at -80°C. Blood for serum ferritin analysis was allowed to clot for 10 minutes, centrifuged for 20 minutes and the serum was aliquoted into fresh tubes for further analysis. Serum collected for analysis of ferritin was analyzed using a ferritin ELISA (ALPCO). Blood samples for oxidative stress measurements were analyzed for reduced glutathione and oxidized glutathione using a microplate assay (Oxford Biomedical Research). To minimize oxidation of reduced glutathione, a thiol scavenger was added immediately to blood samples after collection.

High Pressure liquid chromatography (HPLC)

Brains were removed and immediately placed onto an ice-cold brain block. Striatal samples were carefully dissected, weighed, and frozen on dry ice for HPLC-EC analysis. Samples were prepared and analyzed using HPLC as described previously (Morris et al., 2008).

Western Immunoblotting

SN samples were carefully dissected from fresh brain, placed into centrifuge tubes, weighed, and frozen on dry ice. A 15x volume of cell extraction buffer (Invitrogen) with protease inhibitor cocktail (400uL, Invitrogen), sodium fluoride (200mM), sodium orthovanodate (200 mM), and phenylmethanesulfonylfluoride (200 mM) was added based on tissue weight. Samples were briefly sonicated and protein extraction was allowed to occur on ice for 1 hour with intermittent vortexing. Tubes were centrifuged at 3,000 × g for 20 minutes to pellet cellular debris. Supernatant was collected into fresh tubes. A Bradford assay was performed

on extracted supernatant to determine protein concentrations. Samples were prepared and analyzed using Western blot as previously described (Morris et al., 2010).

Statistical Analyses

Data for glucose tolerance were analyzed using two-way analyses of variance (ANOVA) with diet as the grouping variable and time as the repeated measure. All other data were analyzed using one-way ANOVA with diet as the grouping variable. Data were considered statistically significant at $p \leq 0.05$.

Results

HF diet induces glucose intolerance and oxidative stress

Initial body weight did not differ significantly between the two groups. As expected, a 12-week HF diet significantly increased body weight ($F=230.90$, $p<0.0001$) and epididymal fat ($F=83.40$, $p<0.001$) compared to a chow diet (Table 2). Food intake also differed between groups: as expected, HF-fed animals consumed more calories per day over the course of the experiment ($F=274.19$, $p<0.0001$; Table 2). We performed an IPGTT to analyze whole body glucose tolerance (Figure 1A). Glucose tolerance differed between groups over the course of the IPGTT ($F=5.496$, $p<0.05$), and HF-fed animals exhibited significantly greater area under the curve (AUC) ($F=5.12$, $p<0.05$; Table 2), indicating impaired glucose tolerance. Fasting blood glucose and serum insulin levels were also significantly higher in the HF group ($F=49.20$, $p<0.001$ and $F=F=9.67$, $p<0.01$, respectively), as increased insulin was not able to compensate for rising glucose levels (Table 2). The homeostatic model assessment of insulin resistance (HOMA-IR) is often used to obtain a global measure of insulin resistance (Wallace et al., 2004). The HOMA-IR is based on combined glucose and insulin values following an IGPTT. As expected, HOMA-IR was significantly increased in HF fed animals, indicating insulin resistance ($F=13.6$, $p<0.01$; Figure 1B). Impaired glucose tolerance was accompanied by increased measures of oxidative stress. HF feeding resulted in a significant decrease in serum reduced glutathione ($F=13.5$, $p<0.01$) and a decreased reduced:oxidized glutathione ratio ($F=5.15$, $p<0.05$), indicating less capacity to combat oxidative stress (Figure 1C, 1D). While these effects are not necessarily novel, they are included here to demonstrate insulin resistance resulting from the model. Serum levels of unacylated ghrelin and SN tissue expression of mitochondrial uncoupling protein 2 (UCP2) were also analyzed (Table 2), but did not differ significantly between groups.

HF diet impairs nigrostriatal DA release

Potassium-evoked striatal DA release was analyzed using *in vivo* electrochemistry. A representative plot of DA responses is shown in Figure 2A. The amplitude of striatal DA release was significantly less in HF-fed animals compared to chow-fed animals for the same KCl volume ($F=16.58$, $p<0.01$; Figure 2B). Signal rise times did not differ between the two groups (Table 2), ruling out possible differences in diffusion as an explanation. Interestingly, the amplitude of striatal DA release was positively correlated with HOMA-IR, as more insulin sensitive animals exhibited greater DA responsiveness ($p<0.01$, Figure 2C).

Measures of DA uptake and turnover are reduced by a HF diet

In addition, DA uptake was markedly slower in HF-fed rats: T_{80} was increased ($F=4.58$, $p<0.05$; Figure 3A), indicating that following HF feeding, the average time required for DA concentration to decay was greater. The effect on DA uptake is also evident when analyzing T_c, or clearance rate, which was decreased ($F=4.73$, $p<0.05$; Figure 3B). There was no statistical difference in DA content between the HF diet and chow diet groups (Figure 3C). However, in HF-fed animals, we observed a robust decrease in the DOPAC/DA ratio, which

indicates decreased DA turnover ($F=5.84$, $p<0.05$; Figure 3D) and is consistent with *in vivo* electrochemical measures.

Iron deposition and transport is increased following HF feeding

The effect of a HF diet on iron deposition was also analyzed (Figure 4A). MRI T2 mapping of the SN revealed a significant difference in T2 values between HF and chow-fed rats ($F=5.14$, $p<0.05$ Figure 4B), indicating increased iron deposition. Altered expression of proteins involved in iron transport was also observed in the SN and further indicates increased iron deposition. The protein transferrin receptor 1 (TfR1) plays a role in cellular iron import, while ferroportin facilitates iron export. In HF-fed animals, ferroportin expression was increased ($F=5.021$, $p<0.05$, Figure 5A), while TfR1 was decreased ($F=4.253$, $p=0.05$, Figure 5B), indicating that the cell may be compensating for increased iron load. We also observed differential expression of DMT1, another protein responsive to iron levels and involved in iron transport ($F=4.50$, $p<0.05$, Figure 5C). The protein transferrin (Tf) was significantly increased in this region ($F=4.42$, $p<0.05$, Figure 6A), and we observed a trend for increased transferritin receptor 2 (TfR2) expression ($p=0.07$, Figure 6B). Finally, we also measured hepcidin, which can regulate iron transport through modification of ferroportin. We observed a small but non-significant decrease in hepcidin expression (Table 2).

To determine whether circulating iron levels contributed to iron deposition, we analyzed levels of ferritin in serum. Serum ferritin did not differ between groups (Figure 7A), so it is unlikely that systemic iron levels were affected by diet. However, insulin signaling through the phosphoinositol 3-kinase (PI3-K) pathway increases cell-surface iron transporter expression and cellular iron transport in adipocytes (Davis et al., 1986, Ko et al., 2001). As an index of the PI3-K pathway, we measured phosphorylation of AKT on residue Ser473, which is representative of AKT activation (Alessi et al., 1996). $pAKT_{ser473}$ was increased in the SN ($F=7.23$, $p<0.05$), indicating increased AKT activation (Figure 7B). Because insulin signaling has been shown to increase iron transport in other tissues, it is possible that increased SN insulin signaling could increase iron transport in this region.

Discussion

In this study, a 12 week HF diet resulted in peripheral insulin resistance and oxidative stress. These changes were accompanied by impaired DA function in the dorsal striatum and impaired SN iron homeostasis. Specifically, *in vivo* electrochemical measures of DA neuron function revealed decreased potassium-evoked DA release, which correlated with the degree of insulin resistance. Further impairment of neuronal function was evident by decreased DA clearance in HF-fed animals compared to chow-fed controls. MRI showed a significant decrease in T2 values in the SN of HF-fed rats, indicating increased iron deposition, and expression of iron transport proteins was affected in the SN. Taken together, we have shown that HF diet-induced insulin resistance contributes to impaired function of nigrostriatal DA neurons and may play a role in increased iron deposition in the SN.

The purpose of this experiment was to sample the dorsal striatum as in previous microdialysis and electrophysiological studies (Stanford et al., 2001, Stanford and Gerhardt, 2004). We selected the dorsal striatum because it receives DA input from the SN, where we measured iron homeostasis. (Macdonald and Monchi, 2011). Our results are the first to demonstrate a substantial detrimental effect of a HF diet on specific parameters of DA function in this region of the nigrostriatal pathway. Stimulation with potassium evokes neurotransmitter release in a calcium-dependent manner, mimicking normal neurotransmission (West and Galloway, 1998). Our *in vivo* electrochemical analysis revealed that potassium-evoked DA release was robustly attenuated in HF-fed rats and

correlated with HOMA-IR: decreased DA release was more evident in animals with a greater degree of insulin resistance. DA uptake was also impaired in HF-fed animals. The time required to clear DA (T_{80}) was significantly increased, while the rate of clearance (T_C) was decreased. Although striatal DA content was not different between groups, striatal DA turnover was substantially decreased, supporting the functional *in vivo* electrochemical measures. The observed attenuation in striatal DA turnover in the nigrostriatal pathway may be a consequence of decreased membrane-associated DA transporter in the striatum (South and Huang, 2008). Our findings of impaired *in vivo* DA function in the dorsal striatum extend previous reports of dietary effects on mesolimbic neurons (nucleus accumbens) in brain slices (Davis et al., 2008, Geiger et al., 2009). In the context of parkinsonism, it is interesting to note that the effects of HF feeding on potassium-evoked striatal DA release and clearance in these young adult rats resemble the effects observed previously in senescent 2-year-old F344 rats (Hebert and Gerhardt, 1998).

Given the importance of iron in PD pathogenesis, MRI T2 mapping was performed to further investigate the effects of HF feeding on iron deposition in nigrostriatal neurons. MRI provides a non-invasive method to investigate iron deposition in PD (Graham et al., 2000, Wallis et al., 2008). Lower T2 values indicate increased iron deposition, as spin dephasing from magnetic fields surrounding iron deposits results in loss of signal (reviewed in (Schenck and Zimmerman, 2004)). It has been shown that iron deposition, as measured by T2 weighted MRI, is increased in many neurodegenerative diseases, including PD, as well as in normal aging (Brass et al., 2006). In our study, MRI revealed significantly lower T2 relaxation times in the SN of HF-fed animals compared to chow-fed animals, indicating increased iron levels. It is established that iron plays a role in the generation of highly reactive radicals through Fenton chemistry and may promote DA auto-oxidation (Bharath et al., 2002). Thus, increased iron deposition may be an early event that contributes to DA neuron dysfunction.

Altered expression of iron transport proteins in the SN provides additional evidence of increased iron deposition. Some proteins are responsive to iron levels and contain an iron response element. If the iron response element is contained in the 3′ untranslated region, the transcript is stabilized in response to low iron or down-regulated in response to high iron levels (Anderson and Vulpe, 2009, Kaur et al., 2009). The iron responsive proteins TfR1 and DMT1 contain an iron response element in the 3′ untranslated region and were decreased in the SN of HF-fed animals. As TfR1 is involved in iron import, increased cellular iron content may contribute to the observed compensatory down-regulation of TfR1 expression in our study. Our observed downregulation of the isoform of DMT1 that contains a 3′ IRE is logical in light of our other findings, but should not be overinterpreted. It has previously been shown that DMT1 expression is increased in the SN of PD patients (Salazar et al., 2008). However, our model is not an overt PD model, as we did not observe any DA depletion. In addition, there are four DMT1 isoforms, two of which do not contain an IRE. In the context of this study, decreased DMT1 can be interpreted as a marker of high iron content but the significance of this decrease remains unknown.

However, if the iron response element is contained in the 5′ untranslated region, translation is blocked in conditions of low cellular iron and increased when iron is abundant (Anderson and Vulpe, 2009). Ferroportin is the primary iron exporter and contains an iron response element in the 5′ untranslated region (Anderson and Vulpe, 2009). Studies have shown increased ferroportin mRNA and protein expression with increased iron (Aydemir et al., 2009, Yang et al., 2002). In our study, ferroportin expression was significantly increased in the SN of HF-fed rats, which is likely to result in increased iron export from the cell. We also measured SN levels of hepcidin, which can control ferroportin through post-translational modification (Nemeth and Ganz, 2006). We observed a non-significant

decrease in hepcidin expression. Although this is in line with our observations of increased ferroportin, the non-significant effect on hepcidin suggests that in our study, control of ferroportin is primarily post-transcriptional, through the IRP/IRE system, rather than post-translational, via hepcidin. The differential regulation of TfR1 and ferroportin may represent a compensatory response by the SN to manage a higher iron load.

One outstanding issue in the field of iron homeostasis is how iron gets transported into mitochondria. Iron transport is essential for mitochondrial function (Richardson et al., 2010), but aberrant mitochondrial iron transport could be detrimental. It has been suggested that mitochondrial iron accumulation increases mitochondrial oxidative damage and dysfunction (Seo et al., 2008), and mitochondrial complex I function is impaired in PD (Beal, 2003, Schapira et al., 1989). One hypothesis regarding mitochondrial iron transport that has gained recent support involves Tf and TfR2. Both Tf and TfR2 are localized to mitochondria in DA neurons, are increased with rotenone treatment, and mediate mitochondrial iron transport (Mastroberardino et al., 2009). We observed a significant increase in Tf and a trend for increased TfR2 expression in the SN of HF-fed rats, which may indicate increased mitochondrial iron transport.

The iron storage protein ferritin can be used to gauge whole body iron levels (reviewed in (Wang et al., 2010)). We measured circulating ferritin to determine if systemic iron levels were affected by diet. Ferritin was not different between groups, so it is likely that tissue-specific iron transport, rather than systemic iron overload, contributes to iron dysregulation in the SN. Our 12-week HF diet resulted in impaired glucose tolerance and peripheral hyperinsulinemia. This is relevant because, interestingly, insulin affects iron metabolism (Fernandez-Real et al., 2002). In fat cells, Tf co-localizes with glucose transporters and insulin-like growth factor receptors in microsomes (Tanner and Lienhard, 1989) and insulin stimulates iron uptake by redistributing Tf receptors to the cell membrane (Davis et al., 1986). Because insulin can cross the blood brain barrier (Banks, 2004) and insulin receptors exist in the SN (Moroo et al., 1994), it is possible that iron transport was altered by the increased insulin levels produced by our HF diet. This is supported by our observation of increased AKT phosphorylation, an indicator of increased insulin signaling, in the SN. Insulin is known to activate (phosphorylate) AKT through the PI3-K pathway, and insulin transport across the blood brain barrier is not saturated at plasma insulin levels observed in this experiment (Baura et al., 1993). Insulin stimulation has been shown to increase presentation of TfR by 60%, and this is likely mediated by PI3-K signaling, as PI3-K inhibition decreases cell surface TfR (Ko et al., 2001).

It should be noted that insulin is usually thought to be beneficial for the brain. Intranasal insulin has been consistently shown to improve memory, and insulin signaling can positively affect cell survival (Benedict et al., 2011, van der Heide et al., 2006). However, the effects of insulin in the brain are complex. Insulin receptor substrate 2 (IRS2), a main modulator of brain insulin signaling, can negatively regulate memory formation (Irvine et al., 2011), and calorie restriction (through decreased IRS2 mediated insulin signaling) has been linked to increased longevity (Taguchi et al., 2007). In the context of Alzheimer's disease, insulin has been shown to increase levels of the amyloid beta 42 (Craft, 2009), possibly by interfering with insulin degrading enzyme, which degrades amyloid beta (Qiu et al., 1997). It is likely that insulin can be detrimental at levels that are either chronically lower or higher than normal. We cannot conclude that insulin itself contributed to increased iron deposition in our study, but it is possible that insulin signaling may play a role in our observations of altered iron homeostasis. It would be interesting for future studies to directly measure the effects of insulin on expression of iron transport proteins in neurons.

Other factors that could compromise the function of DA neurons in the nigrostriatal pathway following HF feeding were also analyzed. Oxidative stress occurs peripherally in response to HF feeding, even prior to the onset of insulin resistance (Matsuzawa-Nagata et al., 2008). We observed a significant decrease in the level of reduced serum glutathione and the ratio of reduced to oxidized glutathione in HF-fed animals compared to the chow group, indicating peripheral oxidative stress. HF feeding increases markers of oxidative stress in multiple brain regions, including the SN (Fachinetto et al., 2005, Morrison et al., 2010, Zhang et al., 2005), so it is likely that oxidative stress was also increased in the SN in our 12-week HF diet model. In line with our findings, oxidative damage decreases dopamine transporter expression and DA metabolite levels (Hatcher et al., 2007) so the contribution of oxidative stress to the observed deficits in DA function cannot be ruled out.

We also measured ghrelin, a hormone affected in obesity. Previous studies indicate that ghrelin can be neuroprotective against DA neuron-specific toxins and that this protection occurs via UCP2 (Andrews et al., 2009, Moon et al., 2009). Since decreased ghrelin could make cells more vulnerable to damage, we measured unacylated ghrelin, the most abundant form of ghrelin in serum (Delhanty et al., 2006) and UCP2 expression in the SN. In our study, we did not observe a significant difference in either ghrelin or UCP2 levels between groups, making it unlikely that decreased ghrelin contributes to the observed alterations in nigrostriatal DA function. One other potential player in our observations, specifically, the observed increase in AKT phosphorylation, is leptin. Leptin levels are elevated with increasing adiposity (Maffei et al., 1995) and both leptin and insulin can affect insulin signaling in neurons (Benomar et al., 2005). We did not measure leptin in this study and cannot discount this hormone as a potential player in our observed effects.

Conclusions

We have shown that HF diet-induced insulin resistance produces profound *in vivo* functional effects on nigrostriatal neurons. HF-fed rats exhibited attenuated DA release and uptake in the striatum, and insulin resistance correlated with decreased DA amplitude. Our findings are the first to characterize nigrostriatal DA function *in vivo* in the context of HF-diet induced insulin resistance. These same nigrostriatal neurons exhibited markers of increased iron deposition and a response to increased iron load in the SN. Although other mechanisms cannot yet be ruled out, alterations in iron homeostasis in response to a HF diet could impact nigrostriatal DA neuron function. These changes may precede neurodegeneration and overt DA depletion. Future studies are needed to further investigate the role of iron and insulin signaling on DA neuron function.

Acknowledgments

We thank Susan Smittkamp and George Quintero for technical assistance. This work was supported by NIH grant AG026491 and P20 RR016475, Kansas Intellectual and Developmental Disabilities Research Center grant HD02528, the Kansas City Area Life Sciences Institute, and predoctoral National Research Service Award NS063492 awarded to J. K. Morris, with core support from MRRC and Hoglund Brain Imaging Center.

References

Abbott RD, Ross GW, White LR, Nelson JS, Masaki KH, Tanner CM, Curb JD, Blanchette PL, Popper JS, Petrovitch H. Midlife adiposity and the future risk of Parkinson's disease. Neurology. 2002; 59:1051–1057. [PubMed: 12370461]

Alessi DR, Andjelkovic M, Caudwell B, Cron P, Morrice N, Cohen P, Hemmings BA. Mechanism of activation of protein kinase B by insulin and IGF-1. Embo J. 1996; 15:6541–6551. [PubMed: 8978681]

Anderson C, Checkoway H, Franklin GM, Beresford S, Smith-Weller T, Swanson PD. Dietary factors in Parkinson's disease: the role of food groups and specific foods. Mov Disord. 1999; 14:21–27. [PubMed: 9918340]

Anderson GJ, Vulpe CD. Mammalian iron transport. Cell Mol Life Sci. 2009; 66:3241–3261. [PubMed: 19484405]

Andrews ZB, Erion D, Beiler R, Liu ZW, Abizaid A, Zigman J, Elsworth JD, Savitt JM, DiMarchi R, Tschoep M, Roth RH, Gao XB, Horvath TL. Ghrelin promotes and protects nigrostriatal dopamine function via a UCP2-dependent mitochondrial mechanism. J Neurosci. 2009; 29:14057–14065. [PubMed: 19906954]

Arvanitakis Z, Wilson RS, Bienias JL, Bennett DA. Diabetes and parkinsonian signs in older persons. Alzheimer Dis Assoc Disord. 2007; 21:144–149. [PubMed: 17545740]

Aydemir F, Jenkitkasemwong S, Gulec S, Knutson MD. Iron loading increases ferroportin heterogeneous nuclear RNA and mRNA levels in murine J774 macrophages. J Nutr. 2009; 139:434–438. [PubMed: 19141705]

Banks WA. The source of cerebral insulin. Eur J Pharmacol. 2004; 490:5–12. [PubMed: 15094069]

Baura GD, Foster DM, Porte D Jr, Kahn SE, Bergman RN, Cobelli C, Schwartz MW. Saturable transport of insulin from plasma into the central nervous system of dogs in vivo. A mechanism for regulated insulin delivery to the brain. J Clin Invest. 1993; 92:1824–1830. [PubMed: 8408635]

Beal MF. Mitochondria, oxidative damage, and inflammation in Parkinson's disease. Ann N Y Acad Sci. 2003; 991:120–131. [PubMed: 12846981]

Benedict C, Frey WH 2nd, Schioth HB, Schultes B, Born J, Hallschmid M. Intranasal insulin as a therapeutic option in the treatment of cognitive impairments. Exp Gerontol. 2011; 46:112–115. [PubMed: 20849944]

Benomar Y, Roy AF, Aubourg A, Djiane J, Taouis M. Cross down-regulation of leptin and insulin receptor expression and signalling in a human neuronal cell line. Biochem J. 2005; 388:929–939. [PubMed: 15715521]

Bharath S, Hsu M, Kaur D, Rajagopalan S, Andersen JK. Glutathione, iron and Parkinson's disease. Biochem Pharmacol. 2002; 64:1037–1048. [PubMed: 12213603]

Brass SD, Chen NK, Mulkern RV, Bakshi R. Magnetic resonance imaging of iron deposition in neurological disorders. Top Magn Reson Imaging. 2006; 17:31–40. [PubMed: 17179895]

Cass WA, Zahniser NR, Flach KA, Gerhardt GA. Clearance of exogenous dopamine in rat dorsal striatum and nucleus accumbens: role of metabolism and effects of locally applied uptake inhibitors. J Neurochem. 1993; 61:2269–2278. [PubMed: 8245977]

Choi JY, Jang EH, Park CS, Kang JH. Enhanced susceptibility to 1-methyl-4-phenyl-1,2,3,6-tetrahydropyridine neurotoxicity in high-fat diet-induced obesity. Free Radic Biol Med. 2005; 38:806–816. [PubMed: 15721991]

Craft S. The role of metabolic disorders in Alzheimer disease and vascular dementia: two roads converged. Arch Neurol. 2009; 66:300–305. [PubMed: 19273747]

Davis JF, Tracy AL, Schurdak JD, Tschop MH, Lipton JW, Clegg DJ, Benoit SC. Exposure to elevated levels of dietary fat attenuates psychostimulant reward and mesolimbic dopamine turnover in the rat. Behav Neurosci. 2008; 122:1257–1263. [PubMed: 19045945]

Davis RJ, Corvera S, Czech MP. Insulin stimulates cellular iron uptake and causes the redistribution of intracellular transferrin receptors to the plasma membrane. J Biol Chem. 1986; 261:8708–8711. [PubMed: 3013860]

Delhanty PJ, van der Eerden BC, van der Velde M, Gauna C, Pols HA, Jahr H, Chiba H, van der Lely AJ, van Leeuwen JP. Ghrelin and unacylated ghrelin stimulate human osteoblast growth via mitogen-activated protein kinase (MAPK)/phosphoinositide 3-kinase (PI3K) pathways in the absence of GHS-R1a. J Endocrinol. 2006; 188:37–47. [PubMed: 16394173]

Eberhardt MS, Engelgau M, Cadwell B. Prevalence of overweight and obesity among adults with diagnosed diabetes--United States, 1988-1994 and 1999-2002. MMWR Morb Mortal Wkly Rep. 2004; 53:1066–1068. [PubMed: 15549021]

Fachinetto R, Burger ME, Wagner C, Wondracek DC, Brito VB, Nogueira CW, Ferreira J, Rocha JB. High fat diet increases the incidence of orofacial dyskinesia and oxidative stress in specific brain regions of rats. Pharmacol Biochem Behav. 2005; 81:585–592. [PubMed: 15936064]

Fernandez-Real JM, Lopez-Bermejo A, Ricart W. Cross-talk between iron metabolism and diabetes. Diabetes. 2002; 51:2348–2354. [PubMed: 12145144]

Geiger BM, Haburcak M, Avena NM, Moyer MC, Hoebel BG, Pothos EN. Deficits of mesolimbic dopamine neurotransmission in rat dietary obesity. Neuroscience. 2009; 159:1193–1199. [PubMed: 19409204]

Graham JM, Paley MN, Grunewald RA, Hoggard N, Griffiths PD. Brain iron deposition in Parkinson's disease imaged using the PRIME magnetic resonance sequence. Brain. 123 Pt. 2000; 12:2423–2431.

Gupte AA, Bomhoff GL, Morris JK, Gorres BK, Geiger PC. Lipoic acid increases heat shock protein expression and inhibits stress kinase activation to improve insulin signaling in skeletal muscle from high-fat-fed rats. J Appl Physiol. 2009; 106:1425–1434. [PubMed: 19179648]

Hatcher JM, Richardson JR, Guillot TS, McCormack AL, Di Monte DA, Jones DP, Pennell KD, Miller GW. Dieldrin exposure induces oxidative damage in the mouse nigrostriatal dopamine system. Exp Neurol. 2007; 204:619–630. [PubMed: 17291500]

Hebert, MA.; Gerhardt, GA. Brain Res. Vol. 797. 1998. Normal and drug-induced locomotor behavior in aging: comparison to evoked DA release and tissue content in fischer 344 rats; p. 42-54.

Hindle JV. Ageing, neurodegeneration and Parkinson's disease. Age Ageing. 2010; 39:156–161. [PubMed: 20051606]

Hoffman AF, Gerhardt GA. In vivo electrochemical studies of dopamine clearance in the rat substantia nigra: effects of locally applied uptake inhibitors and unilateral 6-hydroxydopamine lesions. J Neurochem. 1998; 70:179–189. [PubMed: 9422361]

Hu G, Jousilahti P, Bidel S, Antikainen R, Tuomilehto J. Type 2 diabetes and the risk of Parkinson's disease. Diabetes Care. 2007; 30:842–847. [PubMed: 17251276]

Hu G, Jousilahti P, Nissinen A, Antikainen R, Kivipelto M, Tuomilehto J. Body mass index and the risk of Parkinson disease. Neurology. 2006; 67:1955–1959. [PubMed: 17159100]

Irvine EE, Drinkwater L, Radwanska K, Al-Qassab H, Smith MA, O'Brien M, Kielar C, Choudhury AI, Krauss S, Cooper JD, Withers DJ, Giese KP. Insulin receptor substrate 2 is a negative regulator of memory formation. Learn Mem. 2011; 18:375–383. [PubMed: 21597043]

Johnson CC, Gorell JM, Rybicki BA, Sanders K, Peterson EL. Adult nutrient intake as a risk factor for Parkinson's disease. Int J Epidemiol. 1999; 28:1102–1109. [PubMed: 10661654]

Kaur D, Lee D, Ragapolan S, Andersen JK. Glutathione depletion in immortalized midbrain-derived dopaminergic neurons results in increases in the labile iron pool: implications for Parkinson's disease. Free Radic Biol Med. 2009; 46:593–598. [PubMed: 19118623]

Ko KW, Avramoglu RK, McLeod RS, Vukmirica J, Yao Z. The insulin-stimulated cell surface presentation of low density lipoprotein receptor-related protein in 3T3-L1 adipocytes is sensitive to phosphatidylinositide 3-kinase inhibition. Biochemistry. 2001; 40:752–759. [PubMed: 11170392]

Logroscino G, Marder K, Cote L, Tang MX, Shea S, Mayeux R. Dietary lipids and antioxidants in Parkinson's disease: a population-based, case-control study. Ann Neurol. 1996; 39:89–94. [PubMed: 8572672]

Macdonald PA, Monchi O. Differential effects of dopaminergic therapies on dorsal and ventral striatum in Parkinson's disease: implications for cognitive function. Parkinsons Dis. 2011; 2011:572743. [PubMed: 21437185]

Maffei M, Halaas J, Ravussin E, Pratley RE, Lee GH, Zhang Y, Fei H, Kim S, Lallone R, Ranganathan S, et al. Leptin levels in human and rodent: measurement of plasma leptin and ob RNA in obese and weight-reduced subjects. Nat Med. 1995; 1:1155–1161. [PubMed: 7584987]

Mastroberardino PG, Hoffman EK, Horowitz MP, Betarbet R, Taylor G, Cheng D, Na HM, Gutekunst CA, Gearing M, Trojanowski JQ, Anderson M, Chu CT, Peng J, Greenamyre JT. A novel transferrin/TfR2-mediated mitochondrial iron transport system is disrupted in Parkinson's disease. Neurobiol Dis. 2009; 34:417–431. [PubMed: 19250966]

Matsuzawa-Nagata N, Takamura T, Ando H, Nakamura S, Kurita S, Misu H, Ota T, Yokoyama M, Honda M, Miyamoto KI, Kaneko S. Increased oxidative stress precedes the onset of high-fat diet-induced insulin resistance and obesity. Metabolism. 2008; 57:1071–1077. [PubMed: 18640384]

Moon M, Kim HG, Hwang L, Seo JH, Kim S, Hwang S, Kim S, Lee D, Chung H, Oh MS, Lee KT, Park S. Neuroprotective effect of ghrelin in the 1-methyl-4-phenyl-1,2,3,6-tetrahydropyridine mouse model of Parkinson's disease by blocking microglial activation. Neurotox Res. 2009; 15:332–347. [PubMed: 19384567]

Moroo I, Yamada T, Makino H, Tooyama I, McGeer PL, McGeer EG, Hirayama K. Loss of insulin receptor immunoreactivity from the substantia nigra pars compacta neurons in Parkinson's disease. Acta Neuropathol. 1994; 87:343–348. [PubMed: 8017169]

Morris JK, Bomhoff GL, Stanford JA, Geiger PC. Neurodegeneration in an animal model of Parkinson's disease is exacerbated by a high fat diet. Am J Physiol Regul Integr Comp Physiol. 2010; 299(4):R1082–90. [PubMed: 20702796]

Morris JK, Zhang H, Gupte AA, Bomhoff GL, Stanford JA, Geiger PC. Measures of striatal insulin resistance in a 6-hydroxydopamine model of Parkinson's disease. Brain Res. 2008; 1240:185–195. [PubMed: 18805403]

Morrison CD, Pistell PJ, Ingram DK, Johnson WD, Liu Y, Fernandez-Kim SO, White CL, Purpera MN, Uranga RM, Bruce-Keller AJ, Keller JN. High fat diet increases hippocampal oxidative stress and cognitive impairment in aged mice: implications for decreased Nrf2 signaling. J Neurochem. 2010; 114:1581–1589. [PubMed: 20557430]

Nemeth E, Ganz T. Regulation of iron metabolism by hepcidin. Annu Rev Nutr. 2006; 26:323–342. [PubMed: 16848710]

Papapetropoulos S, Ellul J, Argyriou AA, Talelli P, Chroni E, Papapetropoulos T. The effect of vascular disease on late onset Parkinson's disease. Eur J Neurol. 2004; 11:231–235. [PubMed: 15061824]

Priyadarshi A, Khuder SA, Schaub EA, Priyadarshi SS. Environmental risk factors and Parkinson's disease: a metaanalysis. Environ Res. 2001; 86:122–127. [PubMed: 11437458]

Priyadarshi A, Khuder SA, Schaub EA, Shrivastava S. A meta-analysis of Parkinson's disease and exposure to pesticides. Neurotoxicology. 2000; 21:435–440. [PubMed: 11022853]

Qiu WQ, Ye Z, Kholodenko D, Seubert P, Selkoe DJ. Degradation of amyloid beta-protein by a metalloprotease secreted by microglia and other neural and non-neural cells. J Biol Chem. 1997; 272:6641–6646. [PubMed: 9045694]

Rajpathak SN, Crandall JP, Wylie-Rosett J, Kabat GC, Rohan TE, Hu FB. The role of iron in type 2 diabetes in humans. Biochim Biophys Acta. 2009; 1790:671–681. [PubMed: 18501198]

Rhodes SL, Ritz B. Genetics of iron regulation and the possible role of iron in Parkinson's disease. Neurobiol Dis. 2008; 32:183–195. [PubMed: 18675357]

Richardson DR, Lane DJ, Becker EM, Huang ML, Whitnall M, Rahmanto YS, Sheftel AD, Ponka P. Mitochondrial iron trafficking and the integration of iron metabolism between the mitochondrion and cytosol. Proc Natl Acad Sci U S A. 2010; 107:10775–10782. [PubMed: 20495089]

Salazar J, Mena N, Hunot S, Prigent A, Alvarez-Fischer D, Arredondo M, Duyckaerts C, Sazdovitch V, Zhao L, Garrick LM, Nunez MT, Garrick MD, Raisman-Vozari R, Hirsch EC. Divalent metal transporter 1 (DMT1) contributes to neurodegeneration in animal models of Parkinson's disease. Proc Natl Acad Sci U S A. 2008; 105:18578–18583. [PubMed: 19011085]

Schapira AH, Cooper JM, Dexter D, Jenner P, Clark JB, Marsden CD. Mitochondrial complex I deficiency in Parkinson's disease. Lancet. 1989; 1:1269. [PubMed: 2566813]

Schenck JF, Zimmerman EA. High-field magnetic resonance imaging of brain iron: birth of a biomarker? NMR Biomed. 2004; 17:433–445. [PubMed: 15523705]

Schernhammer E, Hansen J, Rugbjerg K, Wermuth L, Ritz B. Diabetes and the Risk of Developing Parkinson's Disease in Denmark. Diabetes Care. 2011

Seo AY, Xu J, Servais S, Hofer T, Marzetti E, Wohlgemuth SE, Knutson MD, Chung HY, Leeuwenburgh C. Mitochondrial iron accumulation with age and functional consequences. Aging Cell. 2008; 7:706–716. [PubMed: 18843794]

South T, Huang XF. High-fat diet exposure increases dopamine D2 receptor and decreases dopamine transporter receptor binding density in the nucleus accumbens and caudate putamen of mice. Neurochem Res. 2008; 33:598–605. [PubMed: 17940894]

Stanford JA, Currier TD, Purdom MS, Gerhardt GA. Nomifensine reveals age-related changes in K(+)-evoked striatal DA overflow in F344 rats. Neurobiol Aging. 2001; 22:495–502. [PubMed: 11378257]

Stanford JA, Gerhardt GA. Aged F344 rats exhibit altered electrophysiological activity in locomotor-unrelated but not locomotor-related striatal neurons. Neurobiol Aging. 2004; 25:509–515. [PubMed: 15013572]

Sulzer D. Multiple hit hypotheses for dopamine neuron loss in Parkinson's disease. Trends Neurosci. 2007; 30:244–250. [PubMed: 17418429]

Swaminathan S, Fonseca VA, Alam MG, Shah SV. The role of iron in diabetes and its complications. Diabetes Care. 2007; 30:1926–1933. [PubMed: 17429063]

Taguchi A, Wartschow LM, White MF. Brain IRS2 signaling coordinates life span and nutrient homeostasis. Science. 2007; 317:369–372. [PubMed: 17641201]

Tanner LI, Lienhard GE. Localization of transferrin receptors and insulin-like growth factor II receptors in vesicles from 3T3-L1 adipocytes that contain intracellular glucose transporters. J Cell Biol. 1989; 108:1537–1545. [PubMed: 2538483]

van der Heide LP, Ramakers GM, Smidt MP. Insulin signaling in the central nervous system: learning to survive. Prog Neurobiol. 2006; 79:205–221. [PubMed: 16916571]

Wallace TM, Levy JC, Matthews DR. Use and abuse of HOMA modeling. Diabetes Care. 2004; 27:1487–1495. [PubMed: 15161807]

Wallis LI, Paley MN, Graham JM, Grunewald RA, Wignall EL, Joy HM, Griffiths PD. MRI assessment of basal ganglia iron deposition in Parkinson's disease. J Magn Reson Imaging. 2008; 28:1061–1067. [PubMed: 18972346]

Wang W, Knovich MA, Coffman LG, Torti FM, Torti SV. Serum ferritin: Past, present and future. Biochim Biophys Acta. 2010; 1800:760–769. [PubMed: 20304033]

West AR, Galloway MP. Nitric oxide and potassium chloride-facilitated striatal dopamine efflux in vivo: role of calcium-dependent release mechanisms. Neurochem Int. 1998; 33:493–501. [PubMed: 10098718]

Xu Q, Park Y, Huang X, Hollenbeck A, Blair A, Schatzkin A, Chen H. Diabetes and risk of Parkinson's disease. Diabetes Care. 2011; 34:910–915. [PubMed: 21378214]

Yang F, Wang X, Haile DJ, Piantadosi CA, Ghio AJ. Iron increases expression of iron-export protein MTP1 in lung cells. Am J Physiol Lung Cell Mol Physiol. 2002; 283:L932–939. [PubMed: 12376346]

York DA, Teng L, Park-York M. Effects of dietary fat and enterostatin on dopamine and 5-hydroxytrytamine release from rat striatal slices. Brain Res. 2010; 1349:48–55. [PubMed: 20599830]

Zhang X, Dong F, Ren J, Driscoll MJ, Culver B. High dietary fat induces NADPH oxidase-associated oxidative stress and inflammation in rat cerebral cortex. Exp Neurol. 2005; 191:318–325. [PubMed: 15649487]

Abbreviations

AUC	Area under the curve
DMT1	Divalent Metal Transporter 1
HF	High Fat
IPGTT	Intraperitoneal glucose tolerance test
MRI	Magnetic Resonance Imaging
PD	Parkinson's disease
PI3-K	Phosphoinositol-3-kinase
Tf	Transferrin

TfR1	Transferrin receptor 1
TfR2	Transferrin receptor 2
UCP2	Uncoupling protein 2
UTR	Untranslated Region

Research Highlights

- High fat-fed animals exhibit attenuated nigrostriatal DA release in vivo
- Nigrostriatal DA release is correlated with the degree of insulin resistance
- Striatal DA uptake and turnover are decreased with high fat feeding
- High fat feeding increases measures of iron deposition in the substantia nigra

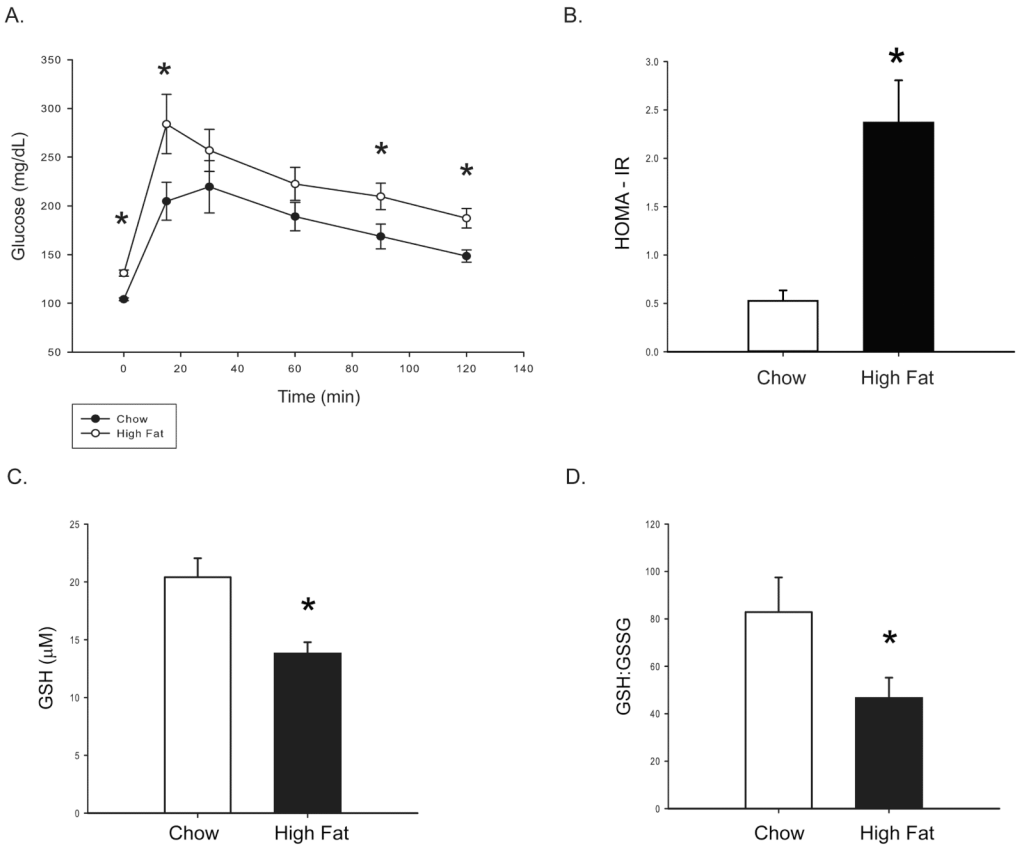

Figure 1. Peripheral glucose tolerance and oxidative stress

After an overnight (12 hour) fast, an intraperitoneal glucose tolerance test was performed. A 60% glucose solution was administered intraperitoneally at 2g glucose/kg body weight. **(A)** Glucose was measured in tail blood at six time points: 0,15,45,60, 90, and 120 minutes after the glucose bolus (injection at t=0). Over the course of the test, glucose levels were higher in HF fed animals. HOMA-IR was also significantly increased **(B)**, indicating insulin resistance. Serum levels of reduced glutathione **(C)** and the ratio of reduced to oxidized glutathione **(D)** were measured to gauge diet-induced oxidative stress. HF-feeding decreased reduced glutathione levels and decreased the ratio of reduced to oxidized glutathione. Values are means ± SE for 11-15 rats per group. *P<0.05 chow vs. HF.

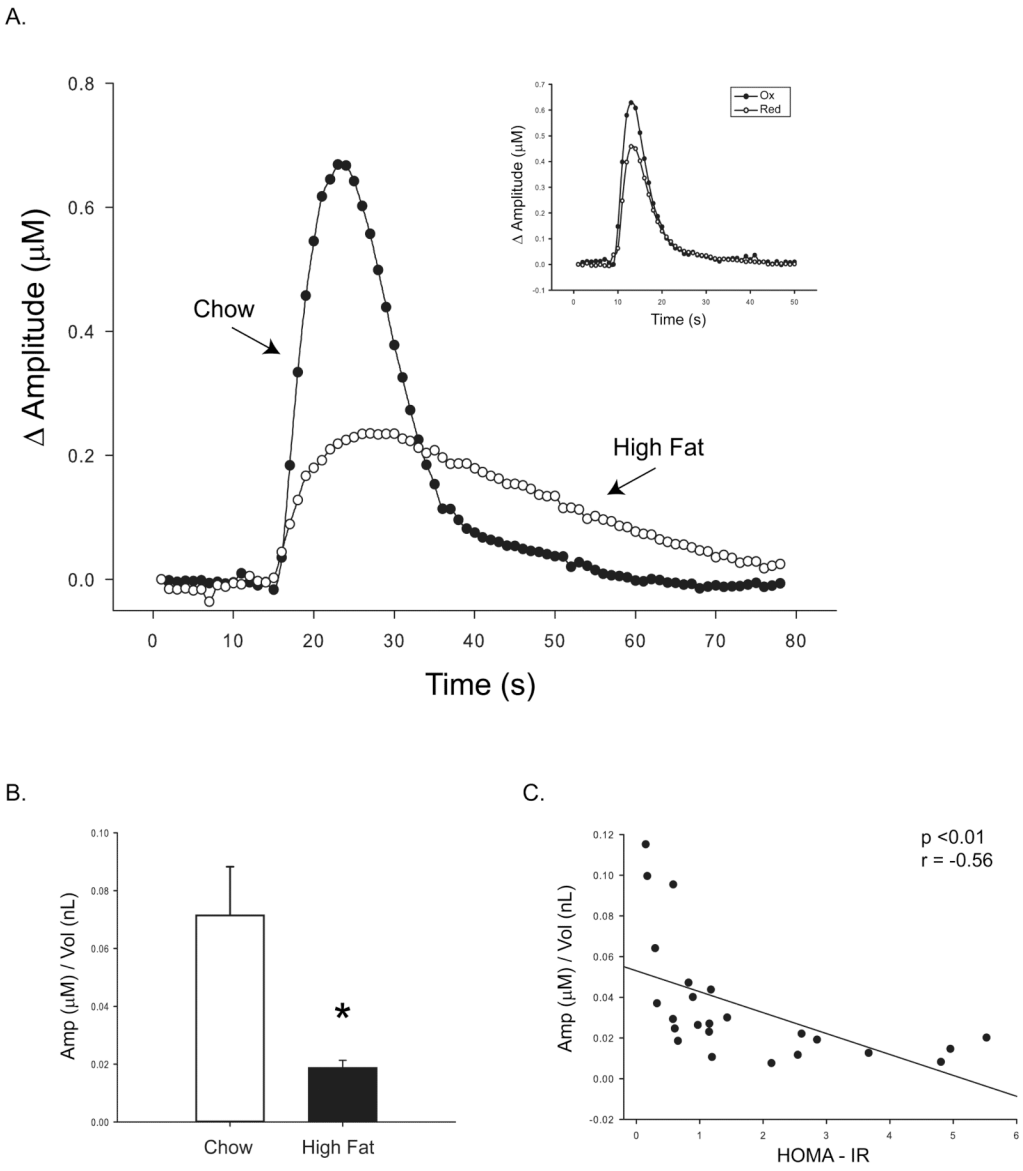

Figure 2. Diet-induced insulin resistance attenuates striatal DA release

In vivo electrochemistry was used to measure potassium-evoked DA release in the striatum. A representative plot of evoked DA signals seen in response to a 50nL KCl stimulus in a HF vs. Chow animal is shown **(A)**. A representative plot of redox ratios indicates specific detection of DA in our study (inset). HF-feeding significantly decreased the amount of DA released per volume of stimulus **(B)**. The degree of insulin resistance (HOMA-IR) correlated negatively with the evoked DA concentration: more insulin resistant animals were less responsive to stimulus **(C)**. Values are means ± SE for 11-15 rats per group. *p<0.05 chow vs. HF.

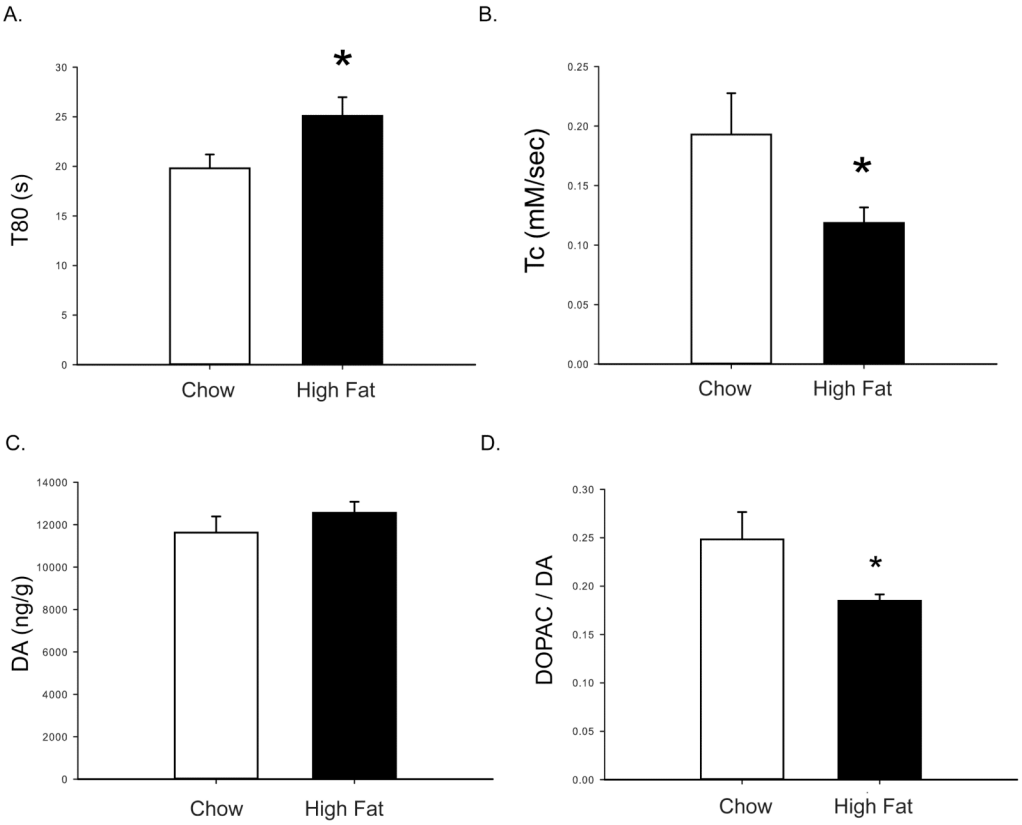

Figure 3. Uptake and turnover mechanics are affected by diet

The rate of DA uptake was also affected by diet. The amount of time required to clear DA (T_{80}) was increased **(A)** and the rate of clearance (T_C) was decreased **(B)** with a HF diet. Although DA content was not affected **(C)**, the DOPAC/DA ratio **(D)**, which indicates decreased DA turnover, was significantly decreased in HF-fed animals. Values are means ± SE for 11-15 rats per group. *p<0.05 chow vs. HF.

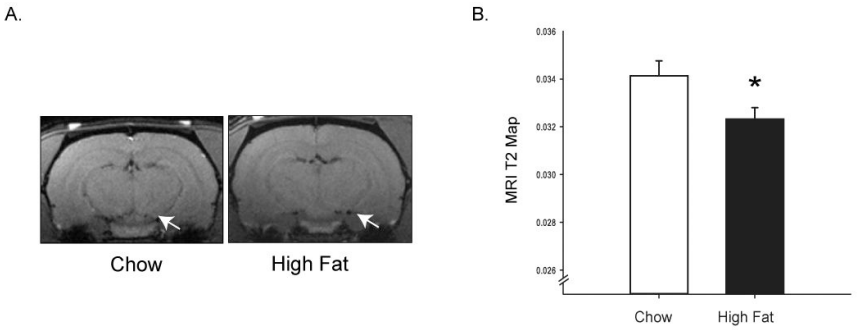

Figure 4. Markers of iron deposition are increased with HF feeding

Magnetic resonance imaging (MRI) was performed on a subset of rats. MRI revealed hypointensity in the SN region, denoted by an arrow **(A)**. T2 values were significantly decreased with a HF diet **(B)**, indicating increased iron deposition. Values are means ± SE for a subset of 3 rats per group for MRI measures. *$p<0.05$ chow vs. HF.

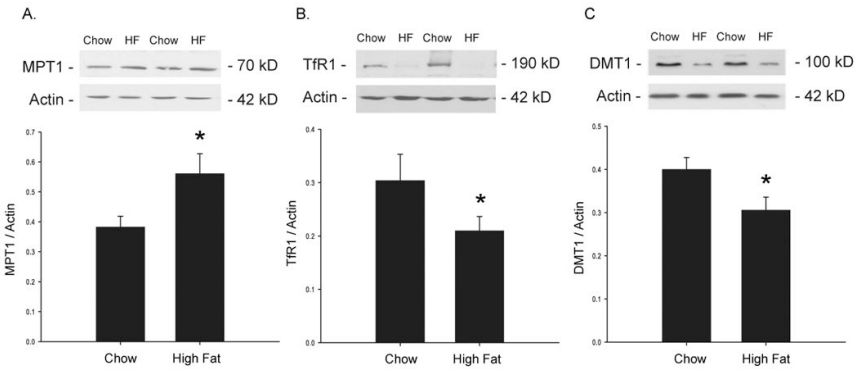

Figure 5. Expression of IRE-regulated proteins in the SN

Expression of proteins involved in iron transport was also affected in the SN. Ferroportin was significantly increased **(A),** while TFR1 **(B)** and DMT1 **(C)** were significantly decreased, suggesting increased intracellular iron content. Values are means ± SE for 11-15 rats per group. *p<0.05 chow vs. HF.

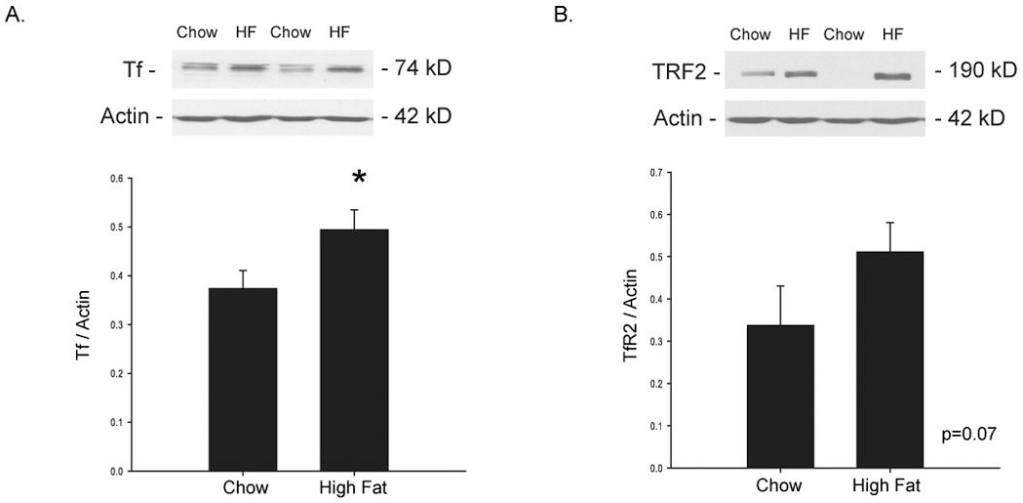

Figure 6. Expression of non-IRE regulated proteins in the SN

The expression of other proteins involved in iron transport was affected as well. Tf was increased **(A)** and a trend for increased TfR2 was observed **(B),** indicating further effects of increased iron. Values are means ± SE for 11-15 rats per group. *p<0.05 chow vs. HF.

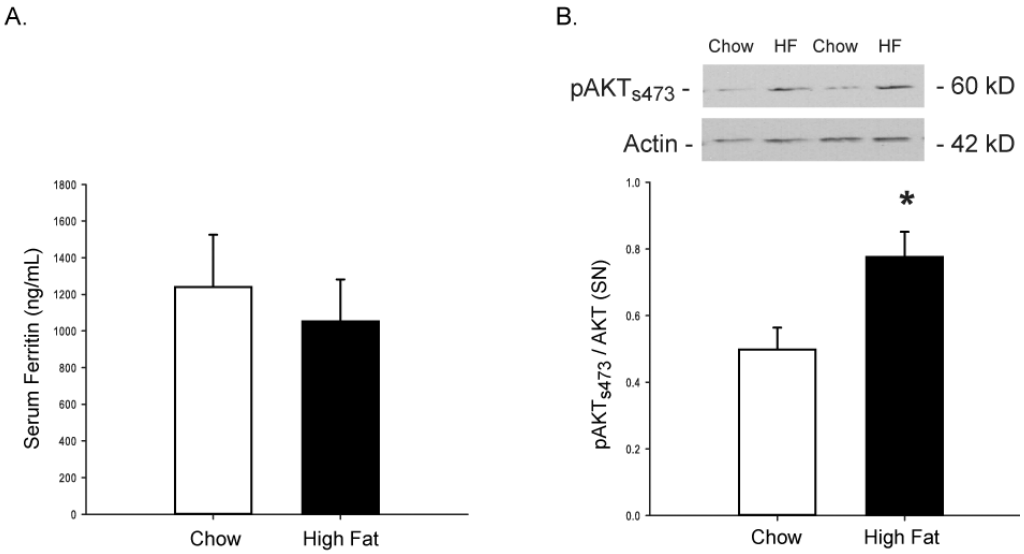

Figure 7. Mechanisms for increased iron deposition

(A) Ferritin levels were not different between groups, indicating that effects on iron transport may be tissue specific and not due to increased circulating iron. Activation of AKT via phosphorylation was analyzed using Western blot **(B)** and indicates upregulation of PI3-K pathway signaling, which has been implicated in iron transport. Serum ferritin levels were analyzed to determine if whole-body iron stores were affected by diet. Values are means ± SE for 11-15 rats per group. *$p<0.05$ chow vs. HF.

Table 1

Ingredient	g/kg
Casein	254
Sucrose	85
Cornstarch	169
Vitamin mix	11.7
Choline Chloride	1.3
Mineral mix	67
Bran	51
Methionine	3
Gelatin	19
Corn oil	121
Lard	218

Table 2

Measure	Chow	High Fat
Final Body Weight (g)	372.1 ± 6.98	483.2 ± 4.19*
Food Intake (kCal / day)	61.3 ± 1.88	71.0 ± 1.49*
Iron intake (mg / day)	5.74 ± 0.057	5.36 ± 0.180*
Epididymal Fat (g)	9.88 ± 0.648	23.35 ± 0.503*
Fasting glucose (mg / dL)	104.8 ± 1.02	131 ± 3.13*
Fasting insulin (μU / mL)	12.15 ± 2.57	44.6 ± 8.48*
Unacylated Ghrelin (pg/mL)	1178.12 ± 87.0	1174.10 ± 42.8
UCP2 (SN)	0.554 ± 0.048	0.533 ± 0.033
Hepcidin (SN)	0.420 ± 0.031	0.360 ± 0.021
Rise time (sec)	12.3 ± 0.950	13.4 ± 0.589
IPGTT Area under curve (AUC)	20913.7 ± 1192	27306.9 ± 2007*

* $p<0.05$